



Seismic performance of ductile welded connections using T-stiffener

M.S. Ghobadi^a, M. Ghassemieh^b, A. Mazroi^c, A. Abolmaali^{d,*}

^a Department of Civil Engineering, Azad University, Qazvin branch, Qazvin, Iran

^b School of Civil Engineering, University of Tehran, Tehran, Iran

^c Department of Civil Engineering, Central Branch of Azad University, Tehran, Iran

^d UT Arlington Center for Structural Engineering Research, University of Texas at Arlington, Arlington, TX, USA

ARTICLE INFO

Article history:

Received 7 March 2008

Accepted 14 May 2008

Keywords:

Connections

T-stiffener

Retrofitting

Ductility

Crack

Weld

ABSTRACT

This study presents the development of the ductile detail of a T-stiffener added to existing moment connections. The seismic behavior of the aforementioned detail was investigated analytically as well as experimentally. A new design criterion is developed for a horizontal element of T-stiffener. Results of this study indicate that the crack propagation is eliminated using the new proposed procedure. This means that by utilizing a fillet weld as a replacement for a CJP groove weld in joining the T-stiffener to a beam flange eliminates crack propagation at the tip of the T-stiffener on the beam flange. In the experimental program, the specimens performed well during the test and reached a total story drift angle of 6% radians before experiencing 20% strength degradation.

Published by Elsevier Ltd

1. Introduction

External T-stiffeners are effective and suitable components for constructing moment-resisting connections with box or concrete filled tube (CFT) columns. Also, the T-stiffener can be used in retrofitting the existing under-designed connection. Fig. 1 illustrates the typical detail of this type of connection and one of its most commonly observed failure modes. There are a number of studies on the behavior of connections and their improvement by the addition of T-stiffeners. Shanmugam et al. [1] and Ting et al. [2] compared the behavior of I-beam to box column connections with different types of external stiffeners using analytical and experimental studies. In their investigations, the connections were subjected to cyclic loadings and their results indicated that using the T-stiffener improves the connection behavior more than the use of external angle stiffeners. The design guidelines for this type of connection were proposed and verified by full scale experiments [3–5]. Also, a number of connections were analyzed by the finite element method for a wide range of dimensions, and the results satisfy the basic design criteria for moment-resisting connections. Similar to the finite element method analysis results, the experimental results indicated that these connections satisfy the basic criteria and provide sufficient strength, stiffness and

rotation capacity. Shin et al. [6] in his study compared both experimentally and analytically the behavior of CFT columns to H beams connections with external T-stiffeners. Three types of failure modes were observed during the tests, including horizontal element failure and vertical element and beam failure. Shin et al. [7] also tested seven CFT beam-to-column connections. To increase ductility and reduce stress concentration at the tip of the horizontal element of the T-stiffener, they implemented RBS cutouts in the beam and drilled a small hole in the horizontal element. Some of the specimens tested demonstrated that the connection can be qualified for special moment-resisting frames in accordance with the AISC seismic provision [8]. However, in some tested specimens, crack propagation was observed. Chen et al. [9] studied the experimental behavior of the reinforced connection with lengthened rib and wing plates. The wing plates are trapezoidal plates which are connected to the beam flange and widen the beam flange at the connection region. In the reinforced connection with wing plates, as in previous research, crack propagation was observed in the tip of the wing plate at the beam flange. Like the horizontal element of the T-stiffener, the wing plate was connected to the beam flange with a CJP groove weld and showed failure modes similar to that of the T-stiffener connection. Yang et al. [10] experimentally compared the cyclic behavior of semi-rigid bolted and fully welded connections. They reported that the fully welded specimen failed due to tearing of the column flange adjacent to the CJP groove weld. Also, the test conducted by Moon et al. [11] revealed that welding failure between the horizontal element of T-stiffener and beam flange triggered the failure of these connections. Mao et al. [12] and Ricles et al. [13,14]

* Corresponding address: UT Arlington Center for Structural Engineering Research, University of Texas at Arlington, 416 Yates 425 Nedderman Hall, 76019-0308 Arlington, TX, USA. Tel.: +1 817 272 3877; fax: +1 817 272 2630.

E-mail address: abolmaali@uta.edu (A. Abolmaali).

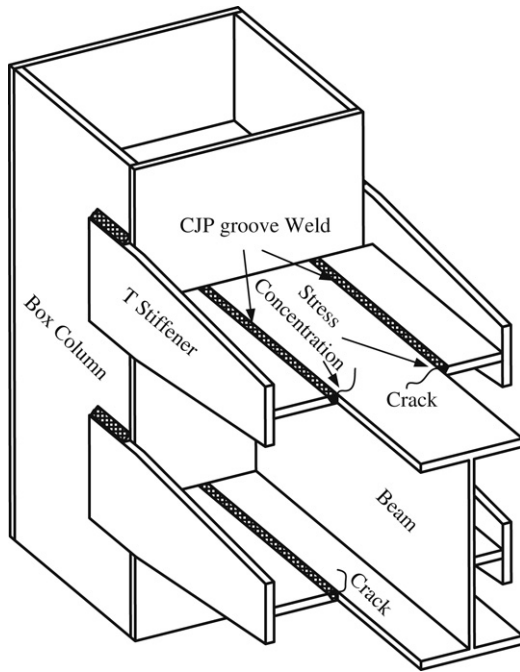


Fig. 1. Moment-resisting connections retrofitted with T-stiffener and its associated failure mode.

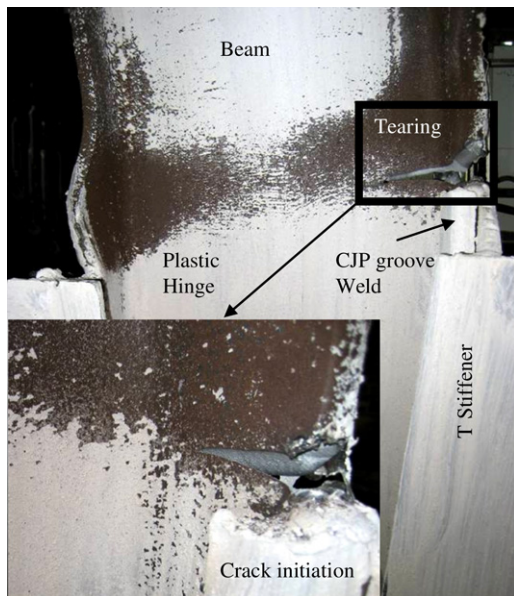


Fig. 2. Observed failure mode in the retrofitted connection with T-stiffener utilizing CJP groove weld to join the horizontal element to the beam flange.

conducted comprehensive experimental and numerical studies in order to provide the ductile detail for welded, non-reinforced moment connections. To develop the study further, the effect of weld metal, weld access hole geometry, beam web attachment, continuity plates and panel zone strength on cyclic ductility were also investigated.

Crack propagation of the T-stiffener was observed at the tip of the horizontal element by Ghobadi et al. [15] (Fig. 2), similar to the studies of the above researchers. They showed that the stress concentration at the heat-affected zone (HAZ) adjacent to the low ductility CJP groove weld causes slight tearing of the beam flange, which ultimately causes failure of the connection. In some cases, tearing of the flange occurs before the 4% story drift ratio

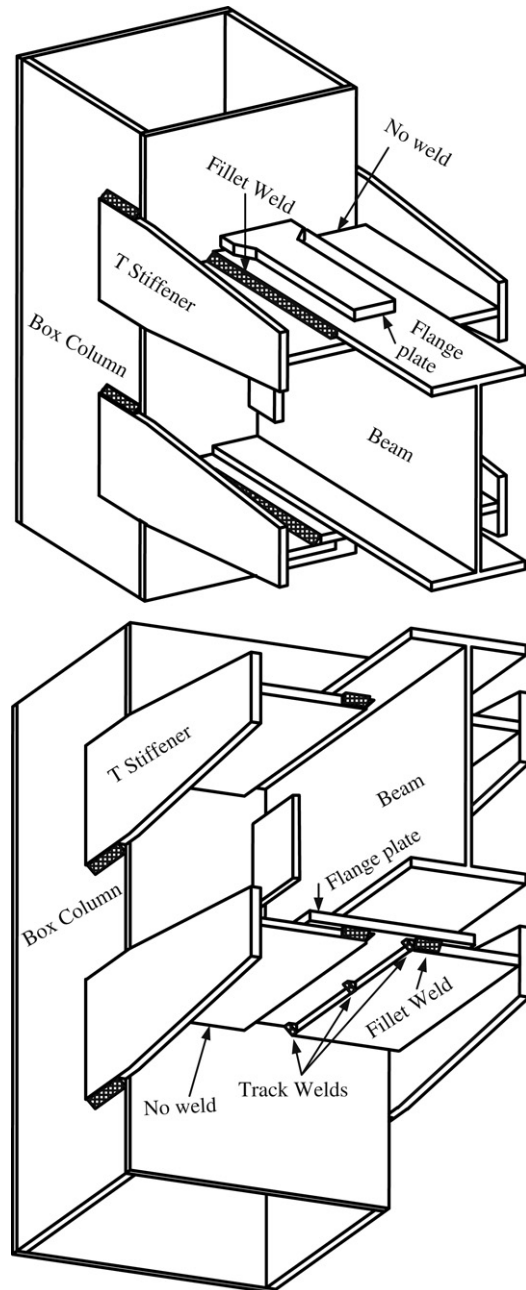


Fig. 3. Proposed joining configuration of the T-stiffener to the flange plate connection, top and bottom view.

is achieved, which results in the failure of the moment-resisting connection before 4% story drift ratio. Hence, it was shown that for a reliable connection, it is much better to eliminate this type of crack propagation in the horizontal element of the T-stiffener.

In the present study, the crack propagation at the tip of the horizontal element of the T-stiffener has been evaluated numerically. Based on the numerical results, a new detail of the joining of the T-stiffener to the beam flange (or flange plate) was developed, which is shown in Fig. 3. This figure shows the fillet welds on the opposite sides of beam flange (or flange plate) are interrupted at the corner of both welds [16]. These types of flange plate connections were tested by Ghobadi et al. [15]. The proposed details for joining the T-stiffener to the existing connections are verified by the nonlinear finite element analysis and experimental tests.

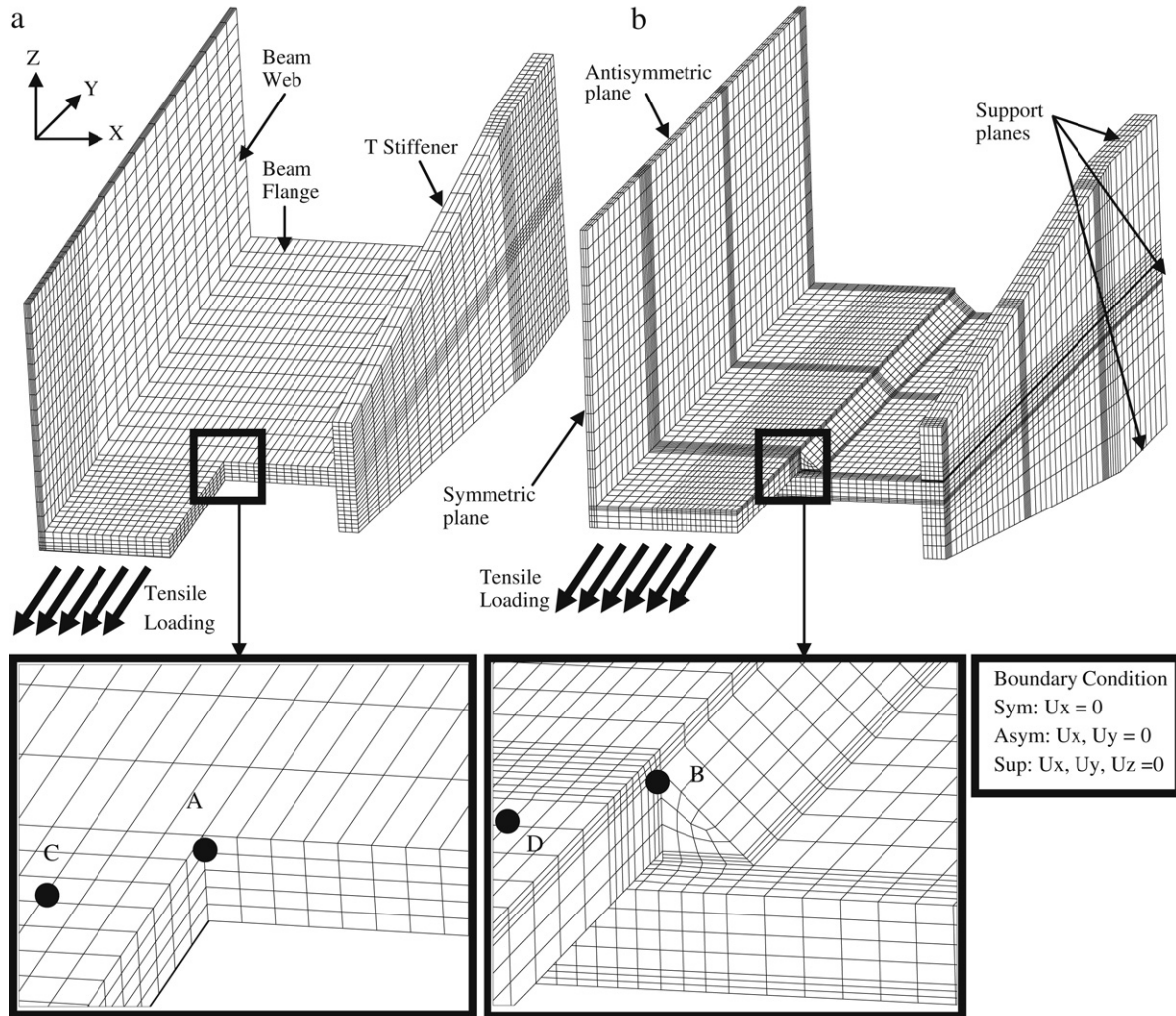


Fig. 4. Finite element model of T-stiffener, a) T-stiffener joined to the beam flange with CJP groove weld, b) T-stiffener joined to the beam flange with fillet weld.

2. Analytical investigation

2.1. Local response of connection

Before performing the full scale experiments, nonlinear 3D finite element (FE) analyses were employed to verify the experimental results and to predict the local behavior of the connection. In the analyses cracks were not explicitly modeled. Two different configurations of the joining of the T-stiffener to the beam flange were considered, including the fillet weld and the CJP groove weld. To evaluate and compare different T-stiffener configurations for ductile fracture potential, a rupture index was used and computed for different cases; this same methodology and approach was used by others [12–14,17]. The rupture index (RI) is defined as:

$$RI = \frac{\varepsilon_p / \varepsilon_y}{\exp(-1.5 \frac{\sigma_m}{\sigma_{eff}})} \quad (1)$$

Where $\varepsilon_p, \varepsilon_y, \sigma_m$ and σ_{eff} are, respectively, the equivalent plastic strain, yield strain, hydrostatic stress, and equivalent stress (also known as the von Mises stress). The large tensile (negative) hydrostatic stress is often accompanied by large principal stresses and generally implies a greater potential for either brittle or ductile fracture. In the presence of a crack or defect, large tensile hydrostatic stress can produce large stress intensity factors at the tip of the crack or defect, and increase the likelihood of brittle fracture [18,19]. The rupture index was introduced by

Hancock and Mackenzie [18] for the equivalent plastic rupture strain of steel for different conditions of stress triaxiality. The process of ductile fracture initiation is caused by a high tensile triaxial stress condition (i.e., high tensile hydrostatic stress), which results in damage accumulation through micro void nucleation and coalescence [18,19]. The ratio of hydrostatic stress to Von Mises stress (σ_m / σ_{eff}) that appears in the denominator of Eq. (1) is called the triaxiality ratio (TR). It was reported [17] that values of TR less than -1.5 can trigger brittle fracture and that values particularly between -0.75 and -1.5 can cause large reductions in the rupture strain of metals. Thus, locations in a connection with higher values of RI have a greater potential for fracture. The ratio of the equivalent plastic strain to yield strain that appears in the numerator of Eq. (1) is called the plastic equivalent strain (PEEQ) index. This index is a measure of the local inelastic strain demand, and is also useful in evaluating and comparing different configurations. The PEEQ index is computed by the following:

$$PEEQ = \frac{\sqrt{\frac{2}{3} \varepsilon_{ij}^p \varepsilon_{ij}^p}}{\varepsilon_y} \quad (2)$$

where ε_{ij}^p are the plastic strain components. The triaxiality ratio and PEEQ index were also computed for different configurations of the T-stiffener joining to provide additional means of comparing the different cases.

In this study, the ANSYS [20] general purpose finite element computer program was used for analyzing the numerical models.

The numerical models and their connection details are shown in Fig. 4. Accordingly, two configurations for joining the T-stiffener to the beam flange are modeled. Four points were selected in order to compare the results of different connection responses, by computing the aforementioned indices for each connection. Points A and B correspond to the same location in different cases, and points C and D are placed in the high plastic stress demand region of the beam flange in the same location for different cases. Three dimensional solid brick elements (SOLID45) were employed to model the structural steel. Both geometric and material nonlinearities are considered in the analyses of the models. Due to symmetry in the plane of the beam web and anti-symmetry in the mid plane of I profile perpendicular to the beam web, and in order to lessen the computational effort, only a quarter section of the specimen was modeled. The T-stiffener connection to the column was considered as a rigid support. The horizontal element of the T-stiffener and beam were not welded to the column flange, and thus were simulated without boundary conditions in the model. In configuration (b), the horizontal elements of the T-stiffener and beam flange are modeled separately with a small space between. These parts are connected to each other with only a fillet weld. Also, the tack welds (shown in Fig. 3) are modeled in configuration (b). The plasticity model was based on the von Mises yielding criterion and its associated flow rule. The fundamental assumptions made to idealize steel mechanical properties were the following: Young's modulus = 2×10^5 MPa, Poisson's ratio = 0.3, yield stress = 320 MPa and tangent modulus = Young's modulus/50. The geometry of both configurations is identical and selected based on the design criteria of the subsequent section.

After analyzing the models, the response indices were computed for points A, B, C and D, as shown in Fig. 5. Comparing the TR indices among the four points revealed that the index at point A was approximately two times that of the other points. This abnormal stress condition adjacent to CJP groove weld (point A) led to the largest reduction of rupture strain among the selected points. The TR index of point B was approximately equal to those of points C and D; this showed that the material behavior adjacent to the fillet weld was similar to the continuous region of beam flange. Furthermore, the TR indices of points A and B suddenly dropped due to the large increase of hydrostatic pressure. The PEEQ index of points indicated that maximum strain demand existed adjacent to the CJP groove weld and minimum strain demand occurred near the fillet weld. The material behavior at points C and D were similar and resulted in equal RI values. Also, the RI of the T-stiffener joining with the CJP groove weld was twice that of the other configuration (i.e., T-stiffener with fillet weld). Thus, when compared to the other configuration, joining the T-stiffener with the fillet weld would have a lower potential for crack initiation. Moreover, the tack welds showed a state of elastic von Mises stress during loading and were found to be safe in configuration (b).

2.2. Design concept of T-stiffener

The connections are designed in accordance with the capacity procedure similar to the work of Shin et al. [6,7]. In calculating the plastic moment capacity of the beam, the strain hardening factor is assumed to be 1.2. The T-stiffener consists of both horizontal and vertical elements. The axial couple force in the beam flange that will be transferred to the column acts as a shear force in the horizontal element and tensile force in the vertical element. In the retrofitted T-stiffener connection, while the vertical element only transfers the load from the beam to the column, the horizontal element plays a more critical role in the ultimate moment and deformation capacity of the connection. Three failure modes were supposed for retrofitted connections: (1) shear failure of the

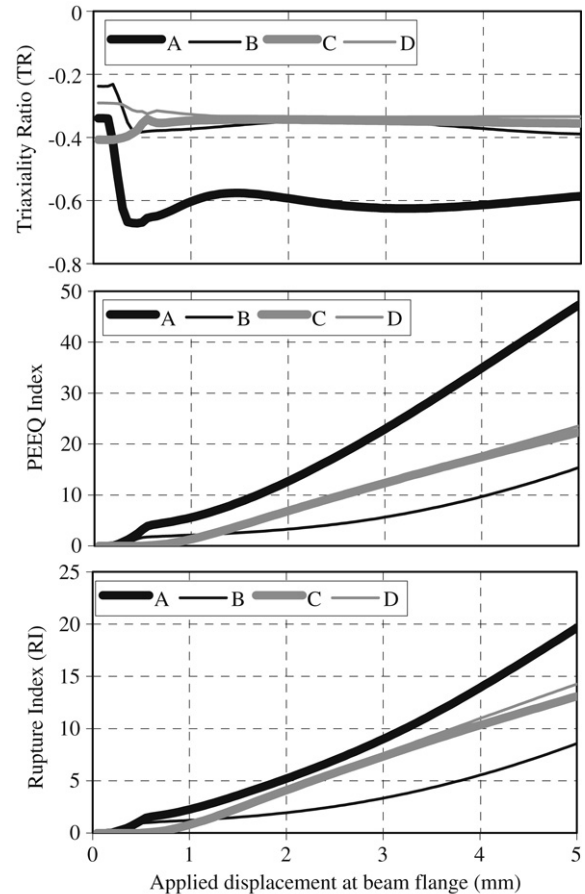


Fig. 5. Response indices of points A, B, C and D vs. applied displacement.

horizontal element; (2) tensile failure of the vertical element at the column web; and (3) bending failure of the beam. Only the failure mode (3) leads to ductile energy dissipation of beam; the other failure modes should not occur in the retrofitted connection. Thus, the design criteria of the T-stiffener should provide safety margins for the desirable behavior of the vertical and horizontal elements. In the tests performed by Shin et al. [6], the connections, TS-3 and TS-6, in which the horizontal element of the T-stiffener had 130% strength relative to the beam flange (strength ratio) for the proposed strength equations, showed stable cyclic behavior and good ductility. In those tests, vertical element had 130% and 100% strength ratios, which showed the design criterion of the vertical element accurately estimated the demands. However, the horizontal element with a 100% strength ratio was not tested. Also, in the next study by Shin et al. [7], the strength ratio of the vertical elements of the T-stiffeners in all specimens were 100%, and the strength ratio of the horizontal elements were 100%, 120% and 140%. The specimens reported having the horizontal element strength ratio of 120% and 140% (i.e., TSD120 and TS140) exhibited excellent performance compared with other specimens. Their results indicated that the horizontal element plays a more effective role than the vertical element in increasing the strength of connections, and the vertical element which was designed based on their proposed criteria shows good performance.

Therefore, after careful inspection of the investigation of other researchers, a rational evaluation is required in order to assess the actual behavior and the load transfer of the horizontal element of the T-stiffener in the connection. Here, the plastic shear strength of the horizontal element was evaluated using nonlinear finite element analysis. The simulated finite element model of the

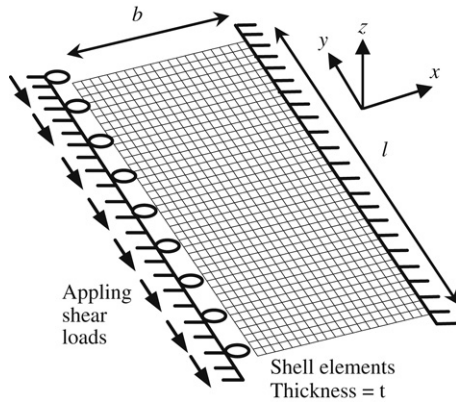


Fig. 6. Modeling of the horizontal element of the T-stiffener.

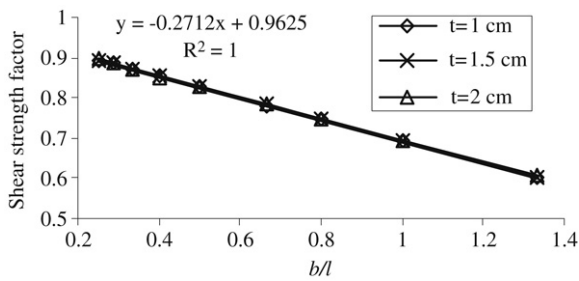


Fig. 7. Aspect ratio effect on the plastic shear capacity of the horizontal element for different thicknesses.

horizontal part of the T-stiffener is shown in Fig. 6. In order to determine the local buckling effect, the specimens were fabricated with an initial imperfection. The effect of residual stress was neglected in the analysis due to the separate fabrication of the T-stiffener and connection. Also when joining the T-stiffener into the connection, the horizontal element is attached first to the beam flange, and the vertical element is attached next to the column flange; thus, the horizontal element does not have significant residual stress. The shear yielding and inelastic shear buckling were two expected failure modes. A total of 27 nonlinear analyses were performed with different aspect ratios and plate thicknesses with the simulated boundary condition of the horizontal element of the T-stiffener. The result indicates that the plastic shear capacity of the plate depends substantially on the aspect ratio of the element as shown in Fig. 7. Also, as indicated, the selected thickness of the plate has no significant effect on the plastic shear strength. The specimen failure modes were dominated by shear yielding, and the large local buckling did not occur in the analyses due to the relatively small size of the plate as compared with the thickness of the plate and the fixed boundary condition of the plate. As illustrated in Fig. 7, the shear strength factor relies alone on the aspect ratio of the horizontal element. Thus, the proposed design criterion of the horizontal element can be considered with the following equation:

$$T_p = M_p / (d - t_f) \tag{3}$$

$$T_p / 2 \leq P_h = \left(0.96 - 0.27 \frac{b}{l} \right) l t_h 0.6 F_{y,h}$$

$$0.25 \leq b/l \leq 1.33 \quad 10mm \leq t_h \tag{4}$$

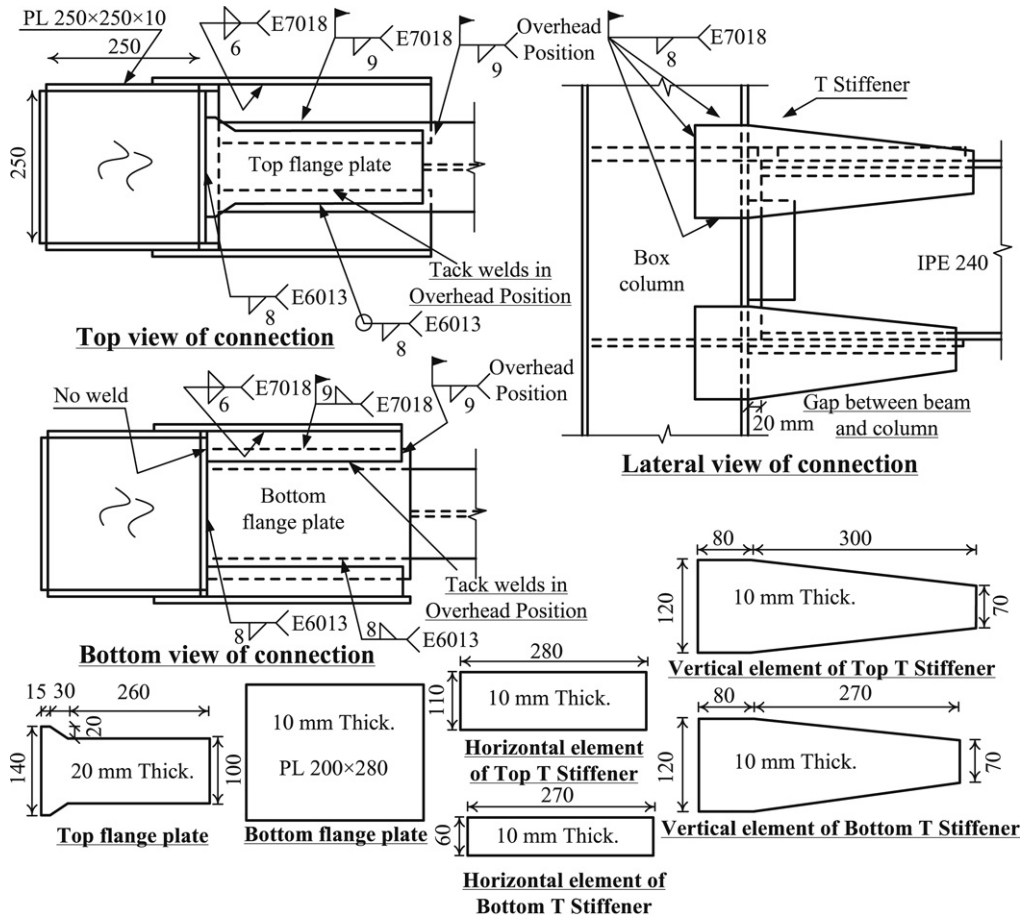


Fig. 8. Connection fabrication details.

